AD

AD-E400-197

CONTRACTOR REPORT ARLCD-CR-78014

EXPLOSIVE HAZARDS TESTS FOR ESTABLISHING HAZARDS CLASSIFICATIONS FOR M1 PROPELLANT FOR AUTOMATED SINGLE-BASE FINISHING OPERATIONS

J. L. EVANS
RADFORD ARMY AMMUNITION PLANT

R. RINDNER
W. SEALS
ARRADCOM

JANUARY 1978

US ARMY ARMAMENT RESEARCH AND DEVELOPMENT COMMAND
LARGE CALIBER
WEAPON SYSTEMS LABORATORY
DOVER, NEW JERSEY

APPROVED FOR PUBLIC RELEASE; DISTRIBUTION UNLIMITED.

Unclassified

SECURITY CLASSIFICATION OF THIS PAGE (When Data Entered)

(19)

REPORT DOCUMENTATION PAGE

READ INSTRUCTIONS BEFORE COMPLETING FORM

1. REPORT NUMBER: ARLCD-CR-78014, AD-E400 197
2. GOVT ACCESSION NO.
3. RECIPIENT'S CATALOG NUMBER (9)
4. TITLE (and Subtitle): (6) EXPLOSIVE HAZARDS TESTS FOR ESTABLISHING HAZARDS CLASSIFICATIONS FOR M1 PROPELLANT FOR AUTOMATED SINGLE-BASE FINISHING OPERATIONS,
5. TYPE OF REPORT & PERIOD COVERED: Final Report. November 1975 - January 1978,
6. PERFORMING ORG. REPORT NUMBER
7. AUTHOR(s): (10) J.L./Evans, Radford Army Ammuniton Plant; R./Rindner, Project Leader, ARRADCOM; W./Seals, Project Engineer, ARRADCOM
8. CONTRACT OR GRANT NUMBER(s): PE-482 (II) (RAD 110.10)
9. PERFORMING ORGANIZATION NAME AND ADDRESS: Radford Army Ammunition Plant, Radford, Virginia 24141
10. PROGRAM ELEMENT, PROJECT, TASK AREA & WORK UNIT NUMBERS: (12) 55p.
11. CONTROLLING OFFICE NAME AND ADDRESS: ARRADCOM, TSD, ATTN: DRDAR-TSS, Dover, NJ 07801 (14) RAD-110.10, PE-482(2)
12. REPORT DATE: (11) January 1978
13. NUMBER OF PAGES: 54
14. MONITORING AGENCY NAME & ADDRESS (if different from Controlling Office): ARRADCOM, LCWSL, MTD, Special Technology Division, Dover, NJ 07801
15. SECURITY CLASS. (of this report): Unclassified
15a. DECLASSIFICATION/DOWNGRADING SCHEDULE
16. DISTRIBUTION STATEMENT (of this Report): Approved for public release, distribution unlimited.

(18) ARLCD, SBIE

17. DISTRIBUTION STATEMENT (of the abstract entered in Block 20, if different from Report)

18. SUPPLEMENTARY NOTES

19. KEY WORDS (Continue on reverse side if necessary and identify by block number)

Vented Vessel
Vent Ratio
Propellant Surface Area
Pressure Relief Venting

20. ABSTRACT (Continue on reverse side if necessary and identify by block number)

Subscale vented vessels of three sizes were tested at various levels of vent areas to determine the effects of vent area and scale (size) on pressurization rates for cannon propellants. Three cannon propellants, M1, M26 and M30 were used in the experimental work; however, only M26 was used to generate data for use in estimating the effects of the above mentioned variables. The overall results were used to predict the pressurization rates resulting from initiation of M26 or M30 propellant in the full-scale AMP dryer. Analyses of the test

DD FORM 1 JAN 73 1473 EDITION OF 1 NOV 65 IS OBSOLETE

Unclassified LB

SECURITY CLASSIFICATION OF THIS PAGE (When Data Entered)

407 057

results and limited mathematical modeling of the pressurization rate in terms of vessel variables indicate that a burning reaction is likely for 680 kg of M26 propellant in this dryer confinement. The properties of M30, relative to M26, indicate that M30 would produce a less severe reaction, under the same conditions as M26 and would, therefore, produce a burning only reaction.

Recommendations were made for continuation of the study, using heavy walled test vessels in order for complete reactions to be achieved under the various degrees of confinement. This program would be concerned with M26 and M-30 cannon propellant testing. The final verification of the modeling approach would require testing of the full scale process vessels.

TABLE OF CONTENTS

TABLES

Page No.

FIGURES

SUMMARY

In this project, tests of subscale vessels simulating the Automated Multi-Base Propellant (AMP) dryer were conducted. Pressure-time data were acquired from the tests and reduced to provide information that could be applied to predicting the in-process hazard classification of the AMP dryer if the M26 or M30 cannon propellant contents were ignited. A limited effort to provide a framework for modeling the reaction process was accomplished.

Although a limited number of tests were conducted under this project, several basic phenomena in the pressurization of vented vessels were identified and demonstrated. Problems with the test system were identified, such as low pressure and weld variability, but were the type problem that could be easily corrected.

INTRODUCTION

In July 1974, Production Engineering Project PE-482 was funded and Phase I studies demonstrated the adequacy of vessel pressure relief venting to preclude an in-process explosion hazard Class 1.1, for 204 kg of M1 propellant in the air dry module discharge hoppers in the Continuous Automated Single-Base Line (CASBL) [1/]. Remaining project funds were diverted and supplemented by additional funds to perform subscale tests and assess the in-process hazard classification during processing of the M26 and M30 cannon propellants in the Continuous Automated Multi-Base Line (CAMBL) propellant dryer [2/]. Presently, this operation is classified as a Class 1.1 mass-detonating hazard because the nitroglycerin content in these compositions is greater than 20 percent [3/]. It is estimated that approximately one million dollars can be saved in facility construction (CAMBL) if the dryer system can be shown to present a Class 1.3 burning hazard. Since full-scale prototype tests were prohibitive from a cost and exposure standpoint, it was discussed and jointly proposed by U. S. Army Armament Research and Development Command (ARRADCOM) and Radford Army Ammunition Plant (RAAP) personnel that subscale tests be conducted to determine the in-process hazard classification of the dryer design when used for drying M26 and M30 propellant.

Initially, the study focused on exploratory tests of M1, M26 and M30 cannon propellants in a vessel of about one-sixth the linear scale of the AMP dryer. The results of these tests were inconclusive; however, they did indicate that modifications could be made in the vessel design to permit the determination of the effects of vessel variables on pressurization parameters. As a result, the study was redirected to test only M26 cannon propellant in vessels simulating 1/4, 1/3 and 1/2 scale models of the AMP dryer. The study was redirected to permit (1) determining the effects of vessel size and vent area on pressurization parameters, (2) a comparison between actual test results and predicted results to determine if data reasonably represented the actual burning process, and (3) limited modeling of the burning reaction in a vented vessel and subsequent prediction of the results of ignition of the contents within the full scale dryer.

1/ Johnson, C. H. and Kristoff, F. T. "Pressure Relief Venting Concept for Eliminating an Explosive Hazard in Continuous Single-Base Operations." Paper presented at 17th DOD Explosives Safety Seminar, Denver, Colorado, September 14-16, 1976.

2/ Letter, Picatinny Arsenal, SARRA-MT-S, dated 28 October 1975

3/ AMCR 385-100

INITIAL EXPERIMENTAL TESTS

Exploratory Tests Utilizing One-Sixth Scale Vessel

The exploratory program to investigate the feasibility of determining the hazard classification of M26 or M30 propellant in the AMP dryer, consisted of testing 25.4 kg of M26 and M30 propellant in a subscale vessel at five levels of vent ratio. Vent ratio is defined as total propellant surface area divided by vessel vent area. Two vent ratio levels were selected above and two below that of the full-scale dryer. The remaining vent ratio was selected to equal 680 kg of M26 propellant in the dryer. The test plan is shown in Table 1. The subscale vessel configuration and dimensions for these tests are shown in Figures 1 and 2, and the full-scale dryer is shown in Figure 3. In addition to the M26 and M30 propellant tests, M1 propellant was tested for purposes of comparison with M26 and M30.

Ignition was accomplished by means of a 12-g bag igniter containing six g of FFFG black powder, six g of ABL 2056D casting powder and one M1 Atlas match, centrally located on the bottom of the vessel. Pressure-time data were acquired from transducers located on each end of the vessel (see Figure 1). A schematic of the data acquisition system is shown in Figure 4.

After analyses of several preliminary tests, the program was expanded to test the higher levels of vent ratio, 781 and 1112, for the M26 propellant formulation in an attempt to achieve higher reaction rates.

Test Results From One-Sixth Scale Vessel

Tests with the one-sixth scale vessel were terminated after analyses of data from 25 trials,which bracketed the dryer vent ratio, indicated that test results would not provide data applicable to mathematical modeling or to determining the probable in-process hazard classification of the AMP drying operation.

The test results are shown in Table 2. After the tests were performed, vessel inspection determined these data to be influenced by leakage of the seal between the hopper body and cover. The magnitude of the effect of leakage could not be determined. Under this condition, the measured effects of vent ratio on pressures obviously contain an unknown error, but the measured pressures could be ranked to show the effects of vent ratio on pressure for the propellants tested in a useable order. For the bolted cover construction, calculations predict approximately 470 kPa would have sheared the lid from the hopper; so it is reasonable to expect that all pressures were below this value. Since the data contained identifiable errors and did not

TABLE 1 - SUB-SCALE TEST PLAN UTILIZING SIXTH-SCALE VESSEL VENT RATIO 1/

Test Level	Vent Area		Propellant Surface Area/Vent Area			Propellant Quantity	
	m^2	(ft^2)	M30	M1	M26	kg/m^2	(lb/ft^2)
1	0.10	(1.12)	141	324	227	250	(50)
2	0.08	(0.86)	184	422	295	323	(65)
3*	0.06	(0.67)	236	542	379	417	(84)
4	0.05	(0.56)	282	648	453	500	(100)
5	0.04	(0.47)	336	773	540	625	(120)

*Level 3 duplicates full-scale AMP dryer conditions

1/ 25 kg (56 lb) propellant employed in above test

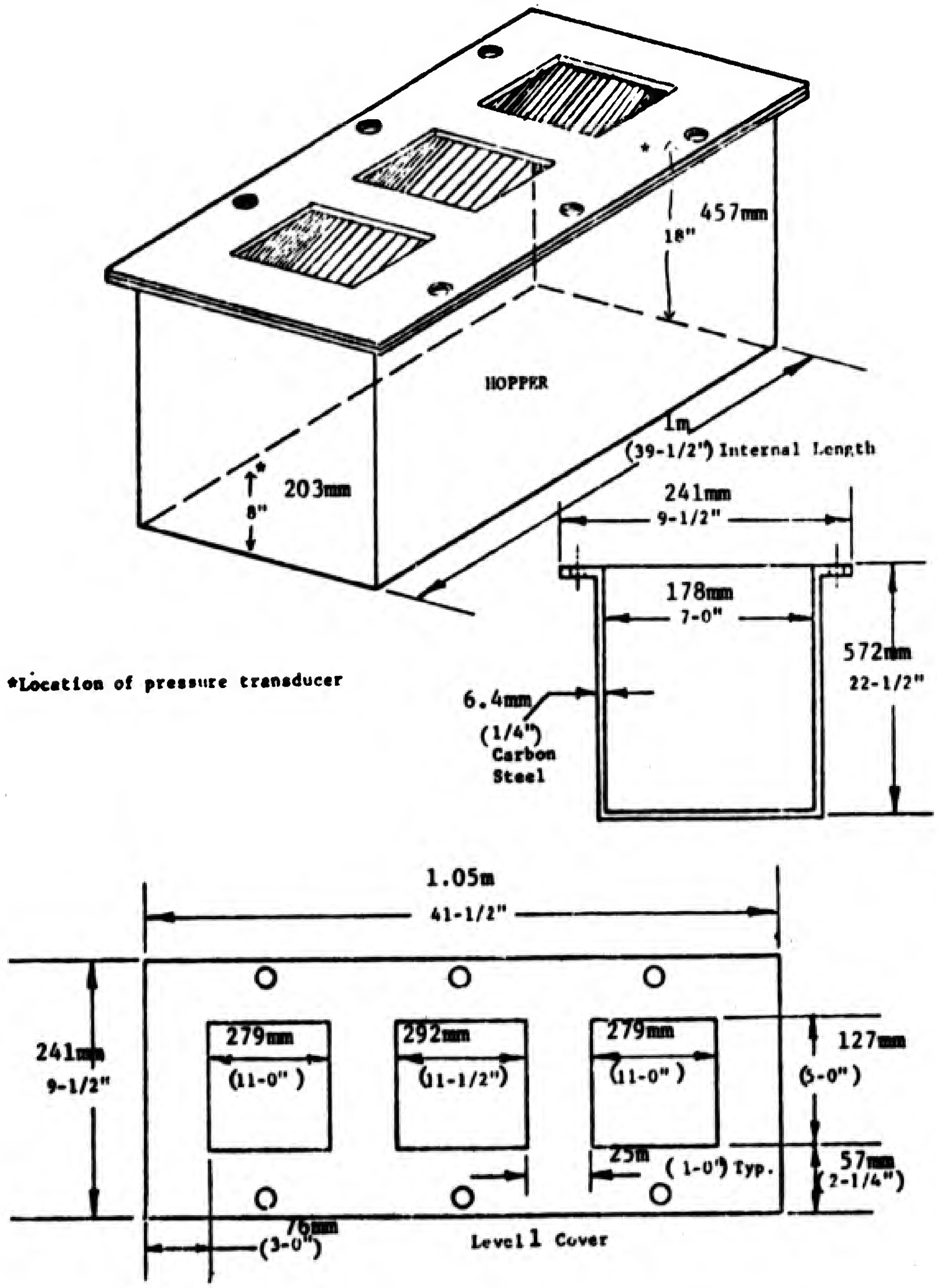

Figure 1. Subscale test vessel (sixth scale) and level 1 vent area cover.

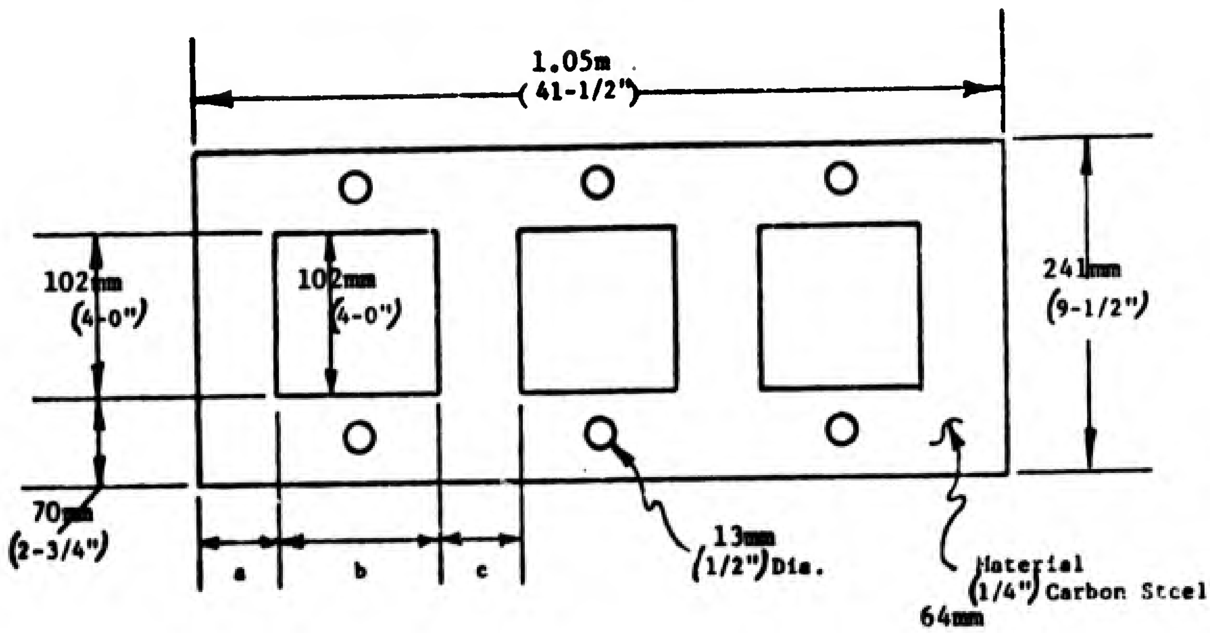

<u>Dimensions 1/</u>

Level	a		b		c	
	mm	in	mm	in	mm	in
2	83	3.25	262	10.33	51	2.00
3	146	5.75	203	8.00	76	3.00
4	168	6.63	172	6.75	102	4.00
5	235	9.25	127	5.00	102	4.00

1/ For vent areas to achieve test levels 2-5 (see Table 1)

Figure 2. Lid dimensions of subscale vessel (sixth scale).

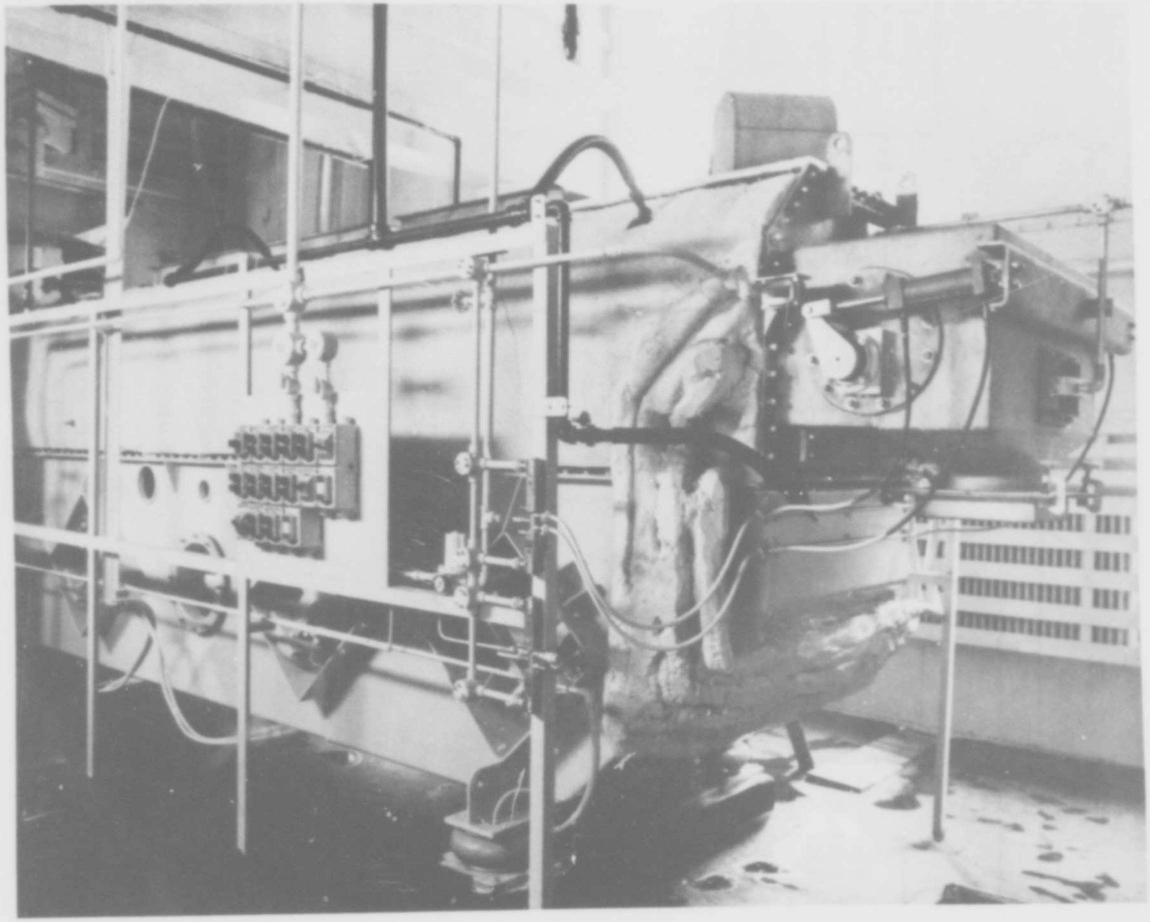

Figure 3. Full scale automated multi-base propellant dryer (Procured from Rexnord, Louisville, KY).

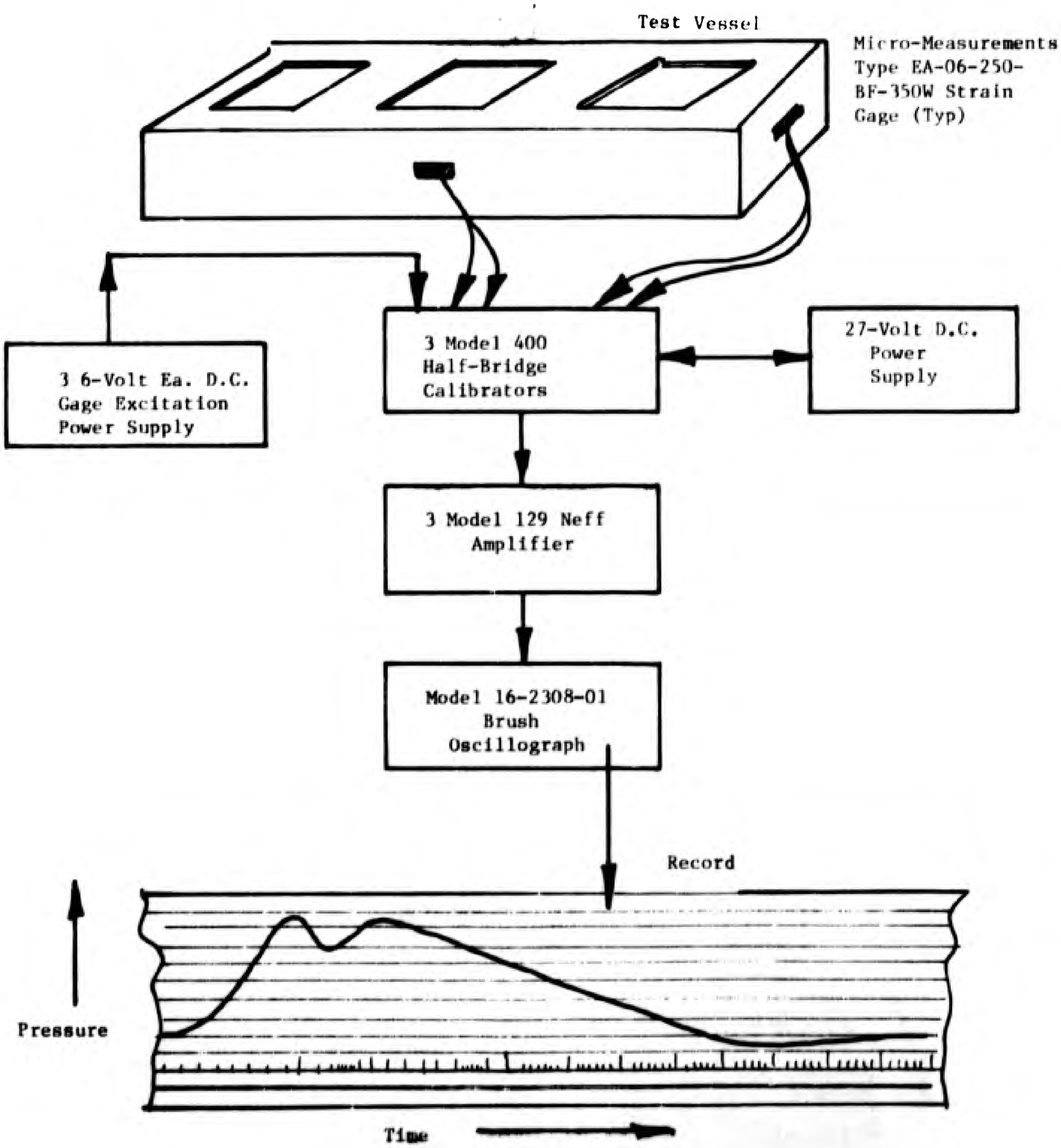

Figure 4. Data acquisition system arrangement.

TABLE 2 - PRESSURE-TIME DATA FOR DIFFERENT VENT RATIOS FOR M1, M26 AND M30 PROPELLANTS, SIXTH SCALE VESSEL

Charge Weight kg	Charge Weight lbs	Vent Ratio	Pressure, Pmax kPa	Pressure, Pmax lbf/in^2	Time to Pmax,s	dp/dt kPa/s	dp/dt $(lbf/in^2)/s$	Remarks
					M1SP			
12.7	28	324	76.5	12.0	0.36	227.1	32.9	
12.2	27	375	47.8	6.9	0.55	86.9	12.6	
25.4	56	773	17.2	2.5	6.40	2.7	0.4	
25.4	56	773	9.9	1.4	0.03 2/	340.0	49.3	
25.4	56	773	7.2	1.3	0.60	15.0	2.2	
25.4	56	773	24.3	3.5	3.00	7.7	1.2	
2.5	5.6	1100	248.2	34.2	0.20	744.6	171.0	
25.4	56	1100	170.7	24.8	0.04 2/	4,477.6	707.4	
					M26			
25.4	56	540	82.5	13.0	1.18	75.8	11.0	
25.4	56	540	91.9	13.3	1.10	83.6	12.1	
25.4	56	769	47.0	6.8	2.15	21.9	3.2	
36.7	81	781	165.6	24.0	--	500.9	72.8	Normal burning,chuffing
36.7	81	781	193.6	28.1	--	430.2	62.4	
36.7	81	1112	185.3	26.9	--	490.9	70.7	Leaked around gasket, normal burning, chuffing
36.7	81	1112	136.3	19.8	--	439.9	63.8	" " "
36.7	81	1112	131.1	19.1	--	439.0	63.7	Damaged cover, leaked; see note
36.7	81	1112	840.0	121.8	--	5,599.9	812.2	Cover blew off
					M30			
11.3	25	150	61.9	8.9	3.60	17.1	2.5	
25.4	56	236	14.3	2.1	9.70	1.4	0.2	
25.4	56	336	31.0	4.5	3.80	7.7	1.2	
25.4	56	336	52.3	7.6	1.50	34.8	5.0	
25.4	56	336	8.4	1.2	1.25	6.8	1.0	
25.4	56	480	26.4	3.8	2.45	10.8	1.6	

1/ Cover increased from 6.4 to 12.7 mm (0.25 to 0.50 in) thickness and sealed with seam sealing compound rather than a neoprene gasket for these tests.

2/ Peak pressure occurred at ignition.

follow a consistent trend, no attempt to model pressure parameters in terms of propellant or vent ratio was made; however, from inspection of the data, the following can be concluded:

1. The long burning times indicate very limited flame propagation through the propellant bed and low burning pressures.

2. Extreme data points show pressures to increase with vent ratio as would be expected.

3. M30 propellant is the least reactive of the three formulations tested.

4. M26 propellant demonstrates a higher reaction rate (or pressurization rate) than either M1 or M30 propellants.

This last conclusion would not necessarily be expected because of the low M26 specific surface but could be explained by relative high pressure exponent compared to M1 or M30 propellant and a somewhat porous bed compared to M1 or M30 propellant (see Appendix A for propellant physical and ballistic properties).

The basic problems with the one-sixth scale vessel design were:

1. The propellant weight was not scaled according to the cube of the scale factor but was selected to be equivalent to the height of propellant in the dryer. The end result produced a loading density up to about 352 kg per cubic meter compared to approximately 192 kg per cubic meter for the AMP dryer.

2. The ignition system employed appeared to provide sufficient force to fluidize the propellant bed and, as a result, produced erratic ignition and, in particular, peak pressure upon ignition. The desired system should provide point ignition and peak pressures after ignition.

3. Flexibility was not provided by the vessel design and any attempted change in vent area or propellant weight to achieve a successful test could not be made in accordance with a given scale factor derived relative to the AMP dryer.

Based on the above, the program was modified to provide (1) test vessels with flexibility, without loss of appropriate scaling, and (2) propellant quantities more closely scaled to the nominal capacity of the AMP dryer. These modifications were made to increase the range of independent variables (vent ratio, size and propellant weight) in order to achieve overall higher pressure parameters and to introduce sufficient spread in the data. The expected net result was that the data would clearly demonstrate trends with the independent variables and, therefore, permit both analyses and modeling of the data. For the modified program, M26 propellant was selected because of the measured higher reaction rates.

EXPERIMENTAL TESTS IN MODIFIED VESSEL

Experimental

The redesigned subscale vessel permitted testing propellant quantities up to 85 kg and was more precisely scaled to AMP dryer dimensions (size and wall thickness) to achieve one-fourth, one-third and one-half scale models (linear dimensions). These yielded propellant weights equivalent to 1/64, 1/27 and 1/8 of the AMP dryer propellant weight when scaled according to the cube of the linear scale factor. The test program for the modified vessel is shown in Figure 5 along with the basic vessel dimensions.

In order to achieve point ignition, these tests utilized two M1 Atlas matches as the ignition source for M26 propellant. The thin-wall design of the test vessels necessitated the use of strain patches bonded to the vessel walls to acquire pressure-time data, rather than pressure transducers which were questionable for this application. Modeling techniques developed by Southwest Research Institute (SWRI) indicated that the strain-time data could be transformed to pressure-time data without loss of accuracy. A discussion of the SWRI model and conversion methods is given in Appendix B. The pressure-time records for these tests were taken from data from strain patches located in the center of the bottom plane and the center of one end and one side of the vessel. The strain-time data were converted to pressure-time data according to the techniques given in Appendix B.

Results of Tests of Modified Vessel

Test Data

The results of M26 propellant tests in the modified vessel are presented in Table 3. With the exception of Test No. 1, which resulted in one end being blown out of the vessel apparently due to a weld defect, all data appeared to follow an expected pattern. Except for three of the one-half scale vessels, all the other vessels failed. Failures were in the weld seam indicating the rupture pressure was controlled by the weld strength. The end weld of the one-half scale vessel is subject to stress of about two times that of the one-fourth scale vessel based on one-half the area of the side plane plus one-half the area of the end plane divided by the height of vessel; thus, if all

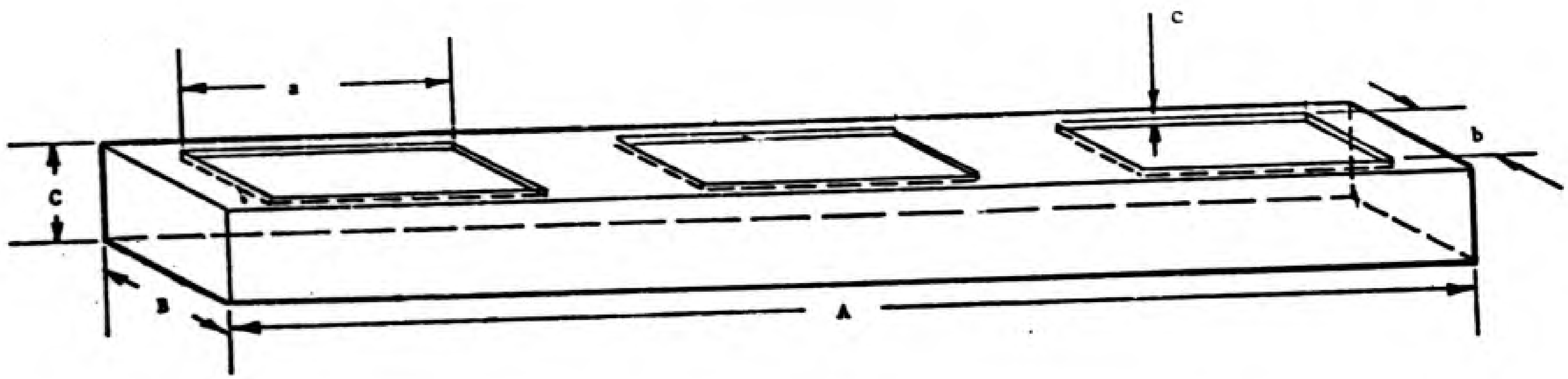

Vessel Scale	Propellant Area, m^2	Vent Ratio	Vent Area, m^2	Dimensions, mm A	B	C	a	b	c
1/4	9.89	800	0.012	1524	248	152	32.5	127	1.6
	9.89	1100	0.009	1524	248	152	23.6	127	1.6
	9.89	1500	0.006	1524	248	152	17.3	127	1.6
1/3	23.4	800	0.029	2032	330	203	77.0	127	1.6
	23.4	1100	0.021	2032	330	203	55.9	127	1.6
	23.4	1500	0.015	2032	330	203	40.9	127	1.6
1/2	79.1	500	0.158	3048	495	305	415.3	127	3.2
	79.1	650	0.122	3048	495	305	319.5	127	3.2
	79.1	800	0.099	3048	495	305	259.3	127	3.2
	79.1	1100	0.072	3048	495	305	188.7	127	3.2
	79.1	1500	0.053	3048	495	305	138.4	127	3.2

Figure 5. Test vessel and nominal dimensions.

TABLE 3 - TEST PARTICULARS AND RESULTS OF SUB-SCALE DRYER TESTS WITH M26 DOUBLE-BASE CANNON PROPELLANT

Test No.	Vessel Scale	Propellant Wt. kg	Propellant Wt. lbs	Propellant, Ht.[1/] mm	Propellant, Ht.[1/] in	Vent Ratio	Time, seconds 0-10% Pmax	Time, seconds 10-90% Pmax	Computed Web Burning Time at Observed Pressure, s	Pressure, Pmax kPa	Pressure, Pmax lbf/in²	Maximum Rate of Pressure, Rise[2/] MPa/s	Maximum Rate of Pressure, Rise[2/] (lbf/in²)/s	Failure Location
1	1/4	10.6	23.44	25-29	1-1.13	800	0.55	0.29	0.37	758	110	8.47	1,229	End
2	1/4	10.6	23.44	25-29	1-1.13	800	0.66	0.13	0.16	2041	296	43.55	6,316	Side and end
3	1/4	10.6	23.44	25-29	1-1.13	1500	0.73	0.22	0.17	1813	263	53.59	7,774[3/]	Side and end
4	1/4	10.6	23.44	25-29	1-1.13	1500	0.99	0.16	0.16	2006	291	51.25	7,433	Side and end
5	1/3	25.2	55.55	38	1.50	1100	0.76	0.15	0.18	1717	249	35.54	5,154	Side
6	1/3	25.2	55.55	38	1.50	1100	-	-	-	-	-	-	-	Record lost, mechanical failure
7	1/2	85.0	187.50	57	2.25	500	0.75	0.70	0.64	510	74	2.87	416[4/]	Did not fail
8	1/2	85.0	187.50	57	2.25	500	0.83	0.97	0.64	524	76	2.94	427[4/]	Did not fail
9	1/2	85.0	187.50	57	2.25	650	0.68	0.60	0.26	1151	167	3.54	513	Did not fail
10	1/2	85.0	187.50	57	2.25	800	-	-	-	-	-	-	-	Record lost, mechanical failure
11	1/2	85.0	187.50	57	2.25	800	0.59	0.35	0.32	889	129	6.55	950	Side
12	1/2	85.0	187.50	57	2.25	1100	0.63	0.23	0.27	1062	154	15.90	2,306	Side

1/ This value varies across the length of the vessel and can only be measured accurately below the vent openings. The measured heights indicate a packing fraction of about 0.577 kg/m^3 (0.036 lbs/in^3).

2/ Maximum occurred from 80-100 percent Pmax, except as noted in 3/ and 4/.

3/ Maximum occurred from 95-100 percent Pmax.

4/ Maximum occurred from 75-90 percent Pmax.

NOTE: Time from 90-100 percent Pmax was $<$ 0.05 seconds in all tests.

welds were of equal quality, the rupture pressure of the one-half scale vessel would be about one-half that of the one-fourth scale vessel. Using this as a criteria, only the above mentioned test (Test No. 1) would be excluded from analyses.

Typical strain-time traces for these tests are shown in Appendix C along with the rationale for selecting regions for rate of pressure rise measurement.

Analysis of Burning Times

In order to determine if the pressure and time parameters adequately represented the actual reaction in the test vessel, computations were made using the rate equation ($r = cp^n$) and physical and ballistic properties of M26 propellant (see Appendix A). Although computations for this type test would not be expected to duplicate actual results, large deviations of actual from expected results would indicate problems with the propellant/vessel system or in the data acquisition system.

The burning rates at the given pressures were computed for each individual test. The corresponding burning times, over the web of the propellant granule, show test burning times to be within about 20 percent of the computed time with the exception of Test Nos. 8 and 9. Assuming the $r = cp^n$ relationship holds at low pressures, two direct conclusions can be drawn, viz., (1) calculated pressures are slightly higher than pressures observed by the propellant, and (2) the propellant bed exhibited to a slight degree, parallel burning rather than burning of all granules simultaneously. The first conclusion indicates pressure deviations from 0 to 152 kPa (using $r = cp^n$ and rate from actual time). The effects of the second conclusion cannot be calculated directly; however, parallel burning over the entire reaction, at the measured pressures, would have produced burning times about 8 to 64 seconds which is several hundred times the actual burning time. This indicates the parallel burning effect is negligible for an M26 propellant bed. Because these conclusions represent extremes, other conclusions such as combined effects, etc., were excluded.

The net result is that the parameters measured from the vessels very likely represent the actual reaction conditions. The effects of the long times from first indication of pressure to ten percent of maximum pressure cannot be determined; however, no more than about 0.44 kg of propellant could have been consumed during this time (based on average pressure of 103 kPa, which corresponds to Test No. 2, the worst case). This reasoning indicates that the measured parameters represent the actual reaction conditions reasonably well (within 10 percent on pressure) and that no selected vessel tested would provide significantly better data than the other two scaled vessels.

Discussion of Data

Relative to the data listed in Table 3, several factors must be considered. These are (1) maximum pressure (a single point measurement) is a function of vessel strength (or quality of weld), (2) rate of pressure rise is measured over a significantly large portion of the pressure-time record (rather than a single point) and is probably established prior to vessel failure, indicating that rate of pressure rise represents the reaction even if the vessel fails, and (3) the total time parameters could vary based on the amount of propellant consumed prior to rupture and, therefore, has a small inherent error.

The data show three trends; namely, (1) maximum pressure increases with vent ratio, (2) rate of pressure rise increases with vent ratio, and (3) for a given vent ratio (unscaled) all parameters, particularly rate of pressure rise, decrease as scale (vessel size) increases. The first two trends are expected. The third trend would not be expected without some mathematical modeling of the propellant/vessel system; however, this trend is critical to safe and functional design of process or test vessels. The rate of pressure rise versus vent ratio curves for the different scales exhibit different slopes, indicating an interaction between vent ratio and scale. The magnitude of this interaction could not be determined because of the limited number of tests conducted; however, the data indicate this interaction to be in a direction to cause the predicted performance to be higher than actual performance in the full-scale dryer.

These parameters are shown as a function of vent ratio in Figure 6 and as a function of vessel scale in Figure 7. Typical results of tests are shown in Figures 8, 9, and 10.

Analysis of AMP Dryer

These test results and their interpretation indicate that a vessel of large size (full scale) with a smaller vent ratio (379) corresponding to 680 kg of propellant in the full-scale AMP dryer would produce a reaction of considerably less severity than any of the sub-scale tests. The estimated reaction pressures would be less than 510 kPa and the rate of pressure rise less than 2.87 MPa/s based on data from one-half scale tests.

From the suggested modeling parameters, Appendix D, relative to scaling vent areas, an estimate of rate of pressure rise in a given scale vessel can be made. If vent areas are scaled according to $(V_{scale}/V_{full})^{2/3}$, vent ratios to produce ideally scaled vessels are obtained, provided all linear dimensions are appropriately scaled. For the vessels tested under this project, all dimensions except vent area, which was dictated by the scope of work, were appropriately scaled.

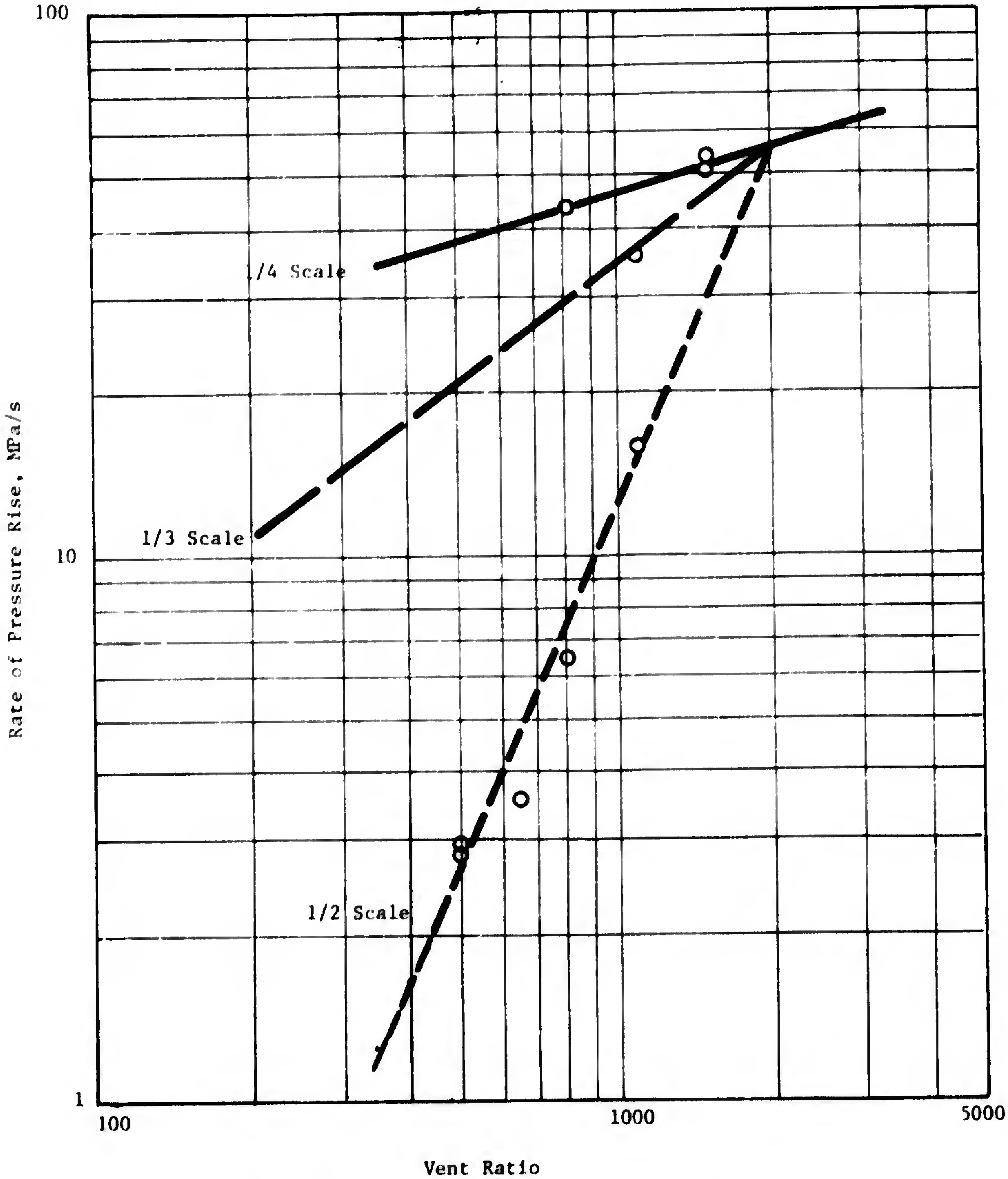

Figure. 6. Rate of pressure rise as a function of vent ratio.

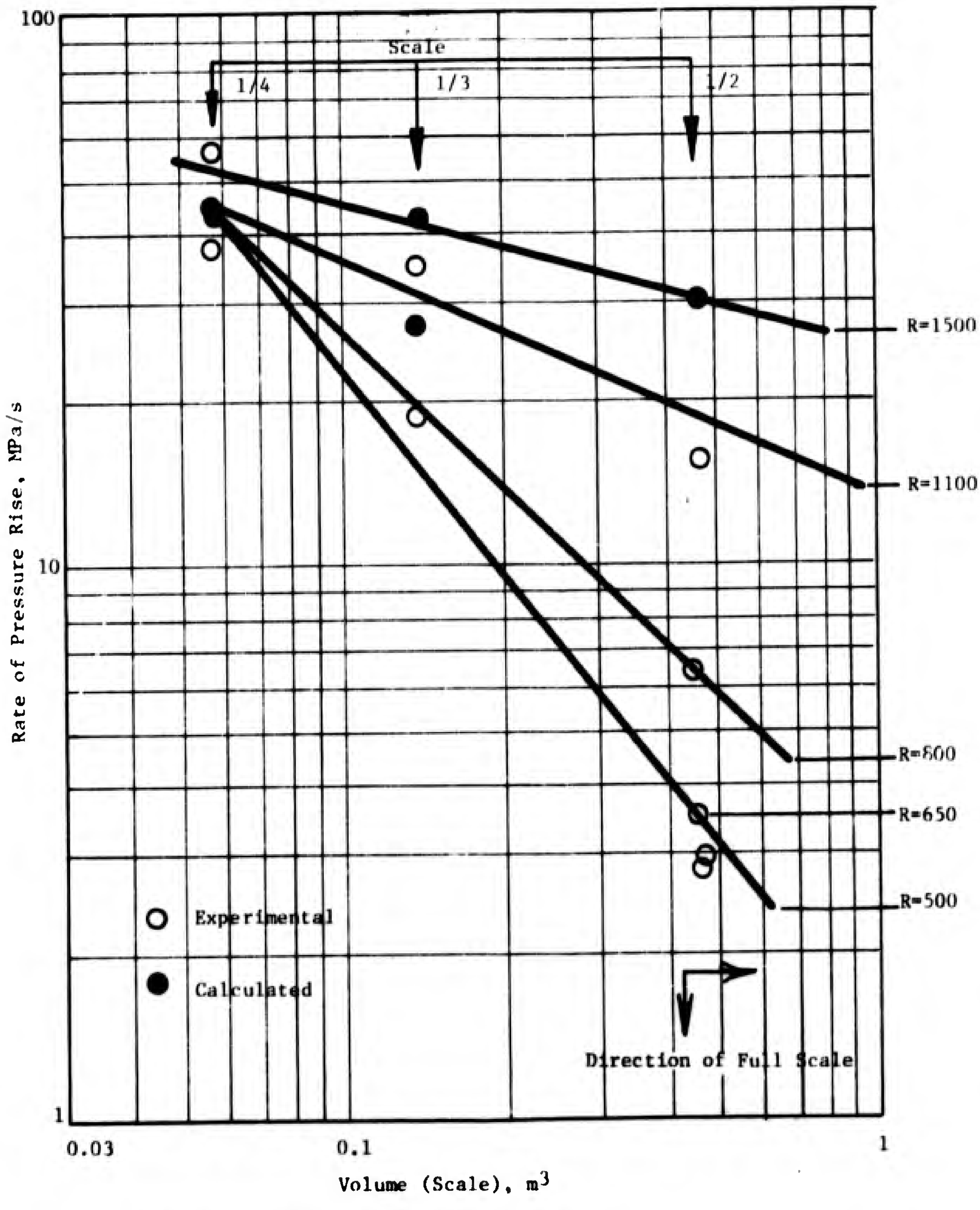

Figure 7. Rate of pressure rise as a function of scale (expressed as volume) based on data from figure 6.

Figure 8. One-half scale test vessel at vent ratio of 500, after test.

Figure 9. One-half scale test vessel at vent ratio of 650, after test.

Figure 10. One-half scale test vessel at vent ratio of 1100, after test.

The scaled vent areas were computed for the one-fourth and one-third vessels based on the one-half scale vessel dimensions (i.e., the one-fourth scale is a half scale of the one-half scale vessel).

The vent ratios corresponding to a vent ratio of 1100 in the one-half scale vessel are 551 and 733 for the one-fourth and one-third scaled vessels, respectively. The rate of pressure rise for these ratios was determined from the lines in Figure 6 and are plotted in Figure 11. This curve demonstrates that pressurization decreases as a vessel increases in size according to a predetermined scale factor. Using a similar argument for the one-half scale vessel relative to the full-scale dryer (vent ratio is 379), a scaled vent ratio of 112 is computed for the one-half scale vessels. This vent ratio predicts a rate of pressure rise of 97 kPa/s (extrapolation from curves in Figure 6) for the one-half scale vessel. This level lies well below the curve shown in Figure 11 and would imply that the full-scale dryer would produce a rate of pressure rise no greater than 97 kPa. A plot of scaled rate of pressure rise as a function of scaled vent area for the vessels tested is shown in Figure 12[1/]. These data are also shown in Table 4. Table 4 shows the parameters for the full-scale dryer. The values for scaled rate of pressure rise was taken from an extrapolation of the curve in Figure 12. This value was used to calculate a rate of pressure rise for the full-scale dryer. The calculated rate of pressure rise is below the observed values for the half-scale tests at vent ratios of 500 and 650, indicating that the AMP dryer should present a burning-only hazards classification of 1.3.

MATHEMATICAL MODELING CONCEPTS

In attempting to model the pressurization event resulting from any cannon propellant reaction in a closed vessel, several factors must be considered. The primary factors are:

1. Propellant reaction rate defined by a burning rate-pressure relationship.

2. Propellant energy, usually defined as heat of explosion per unit weight.

3. Vessel size - volume and cross sectional area.

4. Free volume, loading density, and total propellant weight.

5. Propellant burning area, usually defined as specific surface.

6. Vessel venting conditions, usually defined as vent area/vessel volume, or vent ratio which is the ratio of total propellant burning area to vent area.

1/ This curve was developed by Dr. W. E. Baker, Southwest Research Institute, San Antonio, Texas.

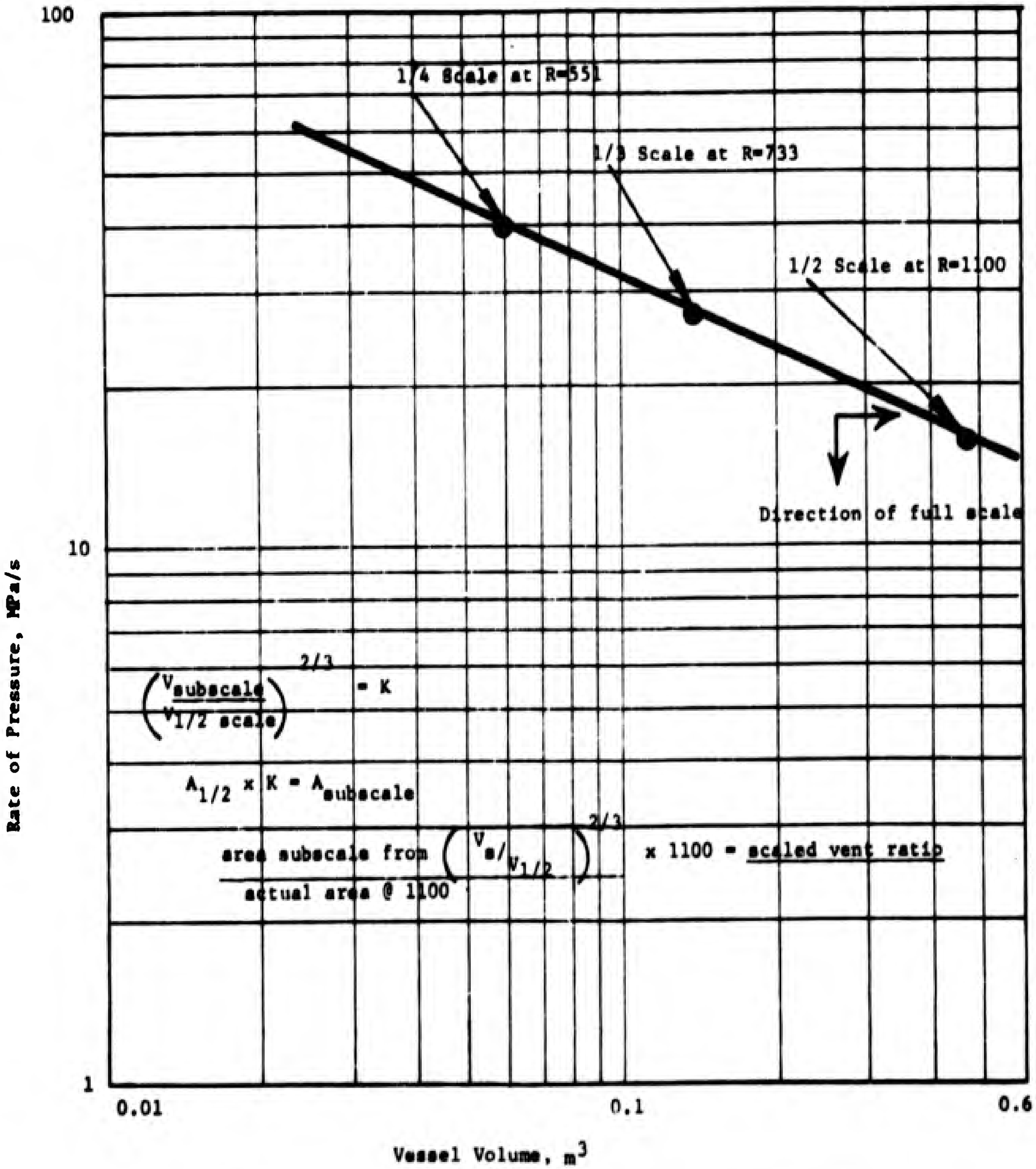

Figure 11 - Rate of pressure rise at scaled vent ratios as a function of vessel volume.

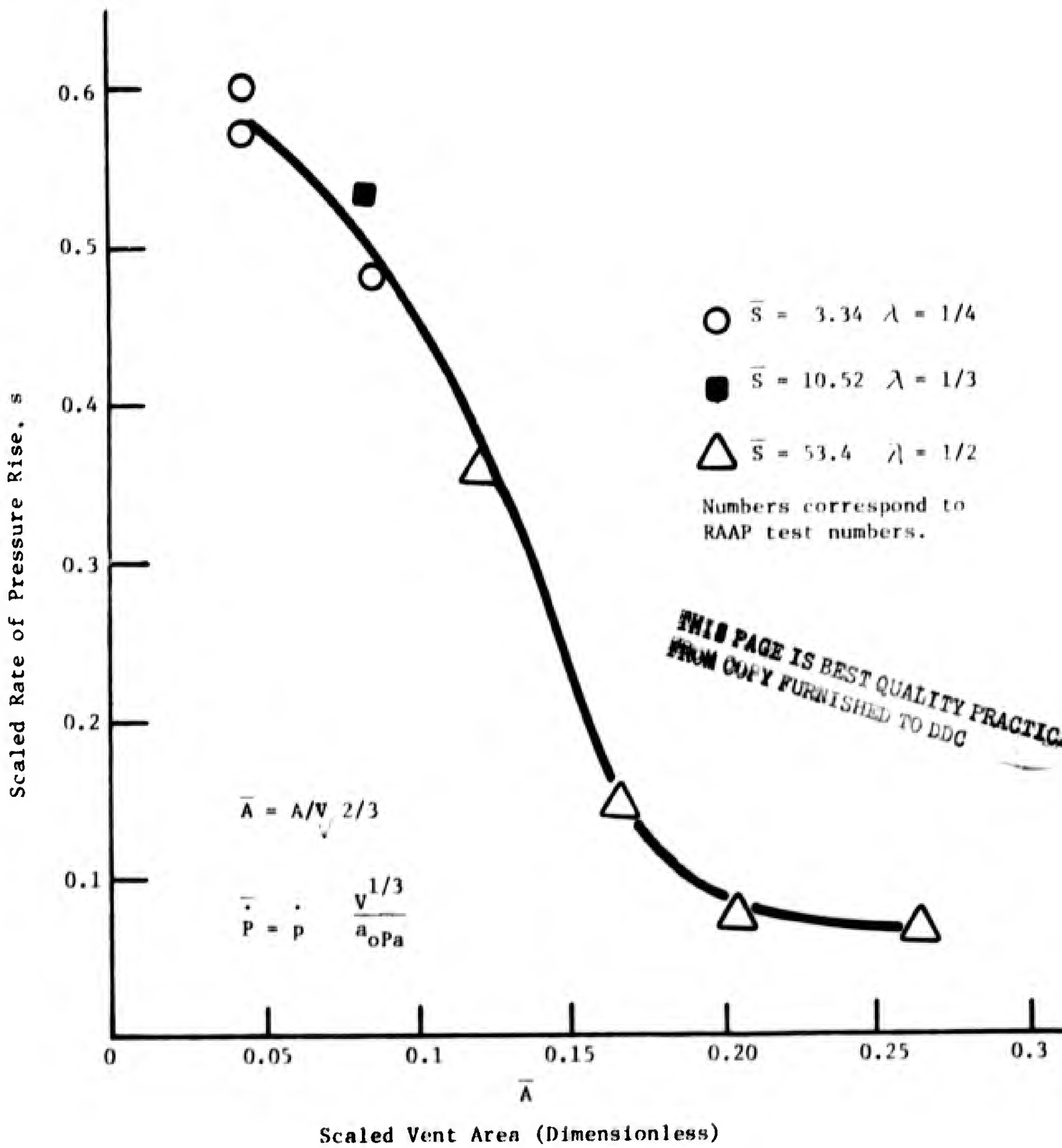

Figure 12 - Scaled maximum pressure rate, M26 propellant in vented chambers.

TABLE 4

SCALED PARAMETERS FOR TEST VESSELS AND TEST RESULTS

Test No.	λ	Prop. Mass, kg	E, MJ	A, m^2	V_v, m^3	S, m^2	pm, kPa	$\dot{p}m$, MPa/s	$\bar{E}$	$\bar{A}$	$\bar{S}$	$\bar{p}$	$\bar{\dot{p}}$
1	1/4	10.6	42.4	0.01238	0.0574	9.89	758	8.47	7.29	0.0832	0.0000334	7.48	0.948
2	1/4	10.6	42.4	0.01238	0.0574	9.89	2041	43.55	7.29	0.0832	0.00334	20.1	0.487
3	1/4	10.6	42.4	0.00659	0.0574	9.89	1813	53.59	7.29	0.0443	0.00334	17.9	0.600
4	1/4	10.6	42.4	0.00659	0.0574	9.89	2006	51.25	7.29	0.0443	0.00334	19.8	0.573
5	1/3	25.2	100.8	0.0213	0.136	23.4	1717	35.54	7.32	0.0805	0.01052	16.9	0.530
6	1/3	25.2	100.8	0.0213	0.136	23.4	--	--	7.32	0.0805	0.01052	--	--
7	1/2	85.0	340	0.158	0.4602	79.1	510	2.87	7.29	0.265	0.0534	5.03	0.0643
8	1/2	85.0	340	0.158	0.4602	79.1	524	2.94	7.29	0.265	0.0534	5.17	0.0658
9	1/2	85.0	340	0.122	0.4602	79.1	1151	3.54	7.29	0.205	0.0534	11.36	0.0793
10	1/2	85.0	340	0.0988	0.4602	79.1	--	--	7.29	0.166	0.0534	--	--
11	1/2	85.0	340	0.0988	0.4602	79.1	889	6.55	7.29	0.166	0.0534	8.78	0.147
12	1/2	85.0	340	0.0719	0.4602	79.1	1062	15.90	7.29	0.121	0.0534	10.48	0.356
Full Scale Dryer	1	680.4	2720.6	1.672	3.6616	633.17	--	--	7.295	0.7013	0.855	6.61 1/	0.03 2/

pa = 101.3 kPa

a_a = 340.3 m/s

e = 4000 kJ/kg

$\bar{A}$ = $A/V_v 2/3$

$\bar{p}$ = p/pa

$\bar{\dot{p}}$ = $(\dot{p}\ V_v 1/3/a_a p_a)$

$\bar{S}$ = $(S\ p_a\ V_v 1/3/a_a^2)$

$\bar{E}$ = $E/p_a\ V_v$

Notes:

1/ Calculated from $\bar{\dot{p}}$ and $\bar{p}$ equation.

2/ Extrapolated from curve in Figure 12.

7. Reaction temperature, normally listed as isobaric or isochoric temperature.

8. Other lesser (because of slight variations among cannon propellants) properties such as ratio of specific heat and heat capacity.

The reaction parameters typically restricted to pressure and time relationships are:

1. Rate of pressure rise, normally computed over a restricted range, such as 10-90 percent maximum pressure, to minimize the effect of variability occurring during ignition and the initial rise in pressure or at the end of burning to eliminate the effect of rapid rises due to propellant breakup or sudden increase in progressivity (exhibited by some multiperforated granules).

2. Maximum pressure over propellant burning region thus excluding known peaks such as ignition spikes.

3. Burning time, usually measured from 10 percent point determined from maximum pressure.

Since modeling efforts related to manufacturing process are almost always initiated from the testing of small-scale vessels, the above must be considered in terms of the scale factor (reduction in size). This factor is defined as the ratio of linear dimensions of the small-scale to the full-scale vessel and, as such, will appear in linear, quadratic or cubic form depending on the vessel/propellant parameter being considered.

The effects of mechanical properties should be excluded from the model, because the mathematical model will predict the outcome of the event in any given vessel. A general rule to follow is perform all tests in a vessel capable of sustaining the pressurization event beyond the completion of the reaction.

The vessel used for subscale tests must be sufficiently large to eliminate wall effects and abnormal fluidization of the bed (if undesired) and small enough to permit pressurization from gas production as well as temperature increases.

The modeling effort on this project was limited because of available time and funds; however, some knowledge about scaling and the magnitude of pressurization parameters was gained. The basic effort under this project was related to estimating the performance of a full scale unit from subscale testing, namely, one-fourth, one-third, and one-half scale models.

To achieve this end, two approaches were possible: (1) simply look at the effects, from a statistically well-designed test, in the form of response surface (use multiple regression), or (2) use a mathematical approach where an element is taken from the full scale unit that contains all the properties of the full scale unit (from the calculus) and assume this element performs identically to the full scale unit. After this, each variable is scaled separately, and parameters are expressed in terms of full scale parameters and a function of the scale factor. This can be represented in the form

$$\phi_F = f(\lambda)\,\phi_S$$

where ϕ_F represents the full scale parameter

ϕ_S represents the subscale parameter

and $f(\lambda)$ represents the scale factor (for the variable scaled) to some power (i.e., $f(\lambda) = \lambda^{1/1}, \lambda^{2/1}, \lambda^{3/1} --- \lambda^{K/n}$

where $K = 1,2,3,$ and $n = 1,2,3$).

The second approach is <u>independent of full scale vessel configuration and propellant formulation</u> which ultimately leads to a <u>basic model</u> representing the reactions under consideration.

Modeling efforts for this project were significantly affected as a result of the venting parameters (vent ratio) being pre-selected and being equal for all scale models tested. As an example, the one-half scale vessel is scaled as λ in the linear dimensions, as λ^2 in cross section, and as λ^3 in propellant weight and volume parameters but vent area is scaled as approximately λ^5 (actually 1/30) rather than λ^2 as would be desired. The net effect of failure to scale vent area is that pressures are higher than would be predicted for proper scaling. Since a true scale model would produce a higher rate of pressure rise, the observed results are in the expected direction.

Comparing the one-fourth and one-half scale vessels, the one-fourth scale is a half-scale model of the half-scale unit but vent area is scaled as one-eighth rather than one-fourth.

Considering $\dot{P}_{1/4} = \frac{1}{\lambda}\dot{P}_{1/2} = 2\dot{P}_{1/2}$

the desired pressure rate of rise would be about 6.89 MPa/s for the one-fourth scale while the actual scale would predict a rate of pressure rise of about 52.4 MPa/s. The actual rate of rise was about 43.4 MPa/s. The difference between predicted and actual 9.0 MPa/s could be accounted for by ignition difference and some variation in free volume (proportionally larger in the one-fourth scale model due to better packing). Representing the one-third scale vessel as a two-thirds scale model of the half-scale vessel, the desired rate of rise would be about 26.9 MPa/s for proper scaling. For the actual scale (1/3.3) the predicted rate of rise is 52.5 MPa/s, the actual rate of rise was 35.5 MPa/s, the difference being influenced by ignition variations.

For the full-scale unit, the predicted rate of rise, from one-half scale tests at a vent ratio of 500, would be less than 138 kPa/s.

The expected relationships between sub-scale and full-scale parameters are detailed in Appendix D.

CONCLUSIONS

The results of the subscale vessel tests were analyzed to determine if the test results represent actual conditions and to determine the relationship between pressurization and vent ratio and vessel size. Conclusions from these analyses are:

1. The measured data represent actual reaction conditions and these test results serve as valid points for assessment of the effects of scale and vent ratio on pressurization parameters.

2. Rate of pressure rise increases as the size of the vessel decreases, within a given vent ratio.

3. Rate of pressure rise increases with vent ratio for a given vessel size.

4. Pressure and burning time varies with vent ratio and scale; however, the magnitude of the effects could not be accurately determined because of the mechanical variables resulting from the thin wall design of the test vessel.

5. Extrapolation of results shows that the AMP dryer should present an in-process burning hazard when processing M26 and M30 propellants. Extrapolation was based on parameters being less than those generated from the one-half scale vessel at a vent ratio of 500.

RECOMMENDATIONS

A follow-on program should be conducted with subscale vessels designed to withstand high pressures (several hundred MPa) in order to obtain complete reaction of all propellant contents. Also, to obtain data necessary for mathematical modeling of the reaction process, several formulations and granulations (Appendix A) should be tested. The resulting pressure-time data would be analyzed in terms of scale, vent ratio, and propellant properties. The model obtained would permit determination of expected events, if a process vessel were ignited, without costly and time-consuming testing. Program documentation detailing the specific tests and propellant formulations to be used has been submitted.

At the completion of the follow-on tests with subscale vessels, full scale tests should be conducted to verify the validity of the modeling approach.

APPENDIX A

PROPERTIES OF CANNON PROPELLANTS USED IN SUBSCALE TESTS

Property	Formulation 1/ M1	M26	M30
Dimension:			
Perforations	1	7	7
L - Length, mm	5.08	11.36	16.82
OD - Outside Diameter, mm	1.143	5.182	7.722
ID - Inside Diameter, mm	0.508	0.457	0.711
W - Web, mm	0.330	0.940	1.473
S - Surface Area per Unit Weight, m^2/kg	4.22	0.92	0.57
ρ - Density, kg/m^3	1569	1619	1661
S/V - Specific Surface, m^{-1}	43.2	9.73	6.22
H_{exp} - Heat of Explosion, J/kg 2/	3.14	4.0	4.3
$(\bar{M}p)g$ - Average Molecular Weight of Products, $\frac{g}{g\text{-mole}}$	22.05	24.06	23.21
T_V - Isochoric Flame Temperature, °C	2144	2803	2767
$(\bar{C}_p)g$ - Heat Capacity at Constant Pressure, J/kg.K	1.83×10^{-3}	1.80×10^{-3}	1.80×10^{-3}
a 3/ - Pressure Coefficient	0.00214	0.00083	0.0057
n 3/ - Pressure Exponent	0.71	0.87	0.65

1/ Formulation refers to ingredients and granulation refers to physical size and design of granules.

2/ Experimental

3/ From $r = ap^n$ at °C (21°)

[redacted]

APPENDIX B

DEFORMATION OF PROPELLANT OVEN UNDER INTERNAL BURNING PRESSURES

Prepared by

Dr. W. E. Baker

Southwest Research Institute
San Antonio, Texas

With Addendum Prepared by

Radford Army Ammunition Plant

DEFORMATION OF PROPELLANT DRYING OVEN UNDER INTERNAL BURNING PRESSURES

W. E. Baker

We have developed design equations for prediction of plastic deformations of a number of structural elements. Several of these can be applied to predicting deformations of the drying oven being used to dry M26 and M30 propellant.

The drying oven is a long, narrow structure, approximately a rectangular box. The models which are contemplated for this structure would be made of formed and welded thin sheet steel. The sides and bottom of the model ovens are therefore thin, long rectangular plates or membranes. The solutions we have developed include deformations of such elements, with both bending and membrane action included. The solutions agree well with experimental data from the literature. They apply for either long-duration pressure loading (quasi-static), or for short duration loading (impulsive). One decides which equation to use depending on whether a characteristic response time for the structure is greater or less than the duration of the pressure.

The design equations are as follows:

For quasi-static pressure loading,

$$\left[\frac{PX^2}{\sigma_y h^2}\right] = \frac{\pi^2}{16}\left[1 + \left(\frac{X}{Y}\right)^2\right] + \frac{\pi^3}{\sqrt{3}}\left[\frac{h}{Y}\right]\left[1 + \frac{X}{Y}\right] + \frac{\pi^4}{128}\left(\frac{w_o}{h}\right)\left[1 + \left(\frac{X}{Y}\right)^2\right] + \frac{\pi^2}{4\sqrt{3}}\left(\frac{w_o}{h}\right)\left[\frac{X}{Y}\right] \qquad (1)$$

and for impulsive loading,

$$\left[\frac{i_r^2 Y^2}{\rho\, \sigma_y h^4}\right] = \frac{1}{2}\left(\frac{w_o}{h}\right)\left[1+\left(\frac{Y}{X}\right)^2\right] + \frac{8\pi}{\sqrt{3}}\left(\frac{w_o}{h}\right)\left[\frac{h}{X}\right]\left[1 + \frac{Y}{X}\right] + \frac{\pi^2}{16}\left(\frac{w_o}{h}\right)^2\left[1+\left(\frac{Y}{X}\right)^2\right] + \frac{2}{\sqrt{3}}\left(\frac{w_o}{h}\right)^2\left(\frac{Y}{X}\right) \qquad (2)$$

Terms in eqs. (1) and (2) are defined as follows:

P = peak quasi-static overpressure (F/L^2)

i_r = reflected blast impulse (FT/L^2)

X = shorter half-span of plate (L)

Y = longer half-span of plate (L)

h = plate thickness (L)

w_o = maximum plate deformation (L)

σ_y = yield stress of plate material (F/L^2)

ρ = density of plate material (FT^2/L^4)

Any consistent set of units can be used in these equations; they are dimensionless.

As an example, let us assume a long-duration pressure loading of 100 psi, and a 1/2-in. mild steel bottom plate on a full-scale oven. Then,

P = 100 psi

X = W/2 = 30/2 = 15 in.

Y = (20 x 12)/2 = 120 in.

h = 0.5 in.

σ_y = 40,000 psi

ρ = 7.36×10^{-4} $lb_f/sec^2/in^4$

We wish to solve eq. (1) for maximum deformation w_o. Substituting the above numbers (all in an inch-lb_f-sec system), we get

$$\left(\frac{100 \times 15^2}{40{,}000 \times 0.5^2}\right) = \frac{\pi^2}{16}\left[1 + \left(\frac{15}{120}\right)^2\right] + \frac{\pi^3}{\sqrt{3}}\left(\frac{0.5}{120}\right)\left(1 + \frac{15}{120}\right)$$

$$+ \frac{\pi^4}{128}\left(\frac{w_o}{0.5}\right)\left[1 + \left(\frac{15}{120}\right)^2\right] + \frac{\pi^2}{4\sqrt{3}}\left(\frac{w_o}{0.5}\right)\left(\frac{15}{120}\right)$$

$$2.25 = 0.6265 + 0.0839 + 1.546\, w_o + 0.3561\, w_o$$

Or,

$$w_o = \frac{(2.25 - 0.6265 - 0.0839)}{(1.546 + 0.3561)} = \underline{\underline{0.809 \text{ in.}}}$$

Therefore, the permanent deformation of a half-inch bottom plate under 100 psi pressure would be a little over 3/4 inch. Equation (2) is applied in a similar manner for short duration loading, but the impulse i_r must be known to predict the loading.

Note that the scaled permanent deformation, (w_o/h), would be exactly the same for scale models of the plate subjected to the same pressure. Actual deformations are smaller for smaller models, in direct proportion to the geometric scale factor λ.

ADDENDUM TO APPENDIX B

This model was used to convert strain-time data to pressure-time data (note time is invariant between the two and needs no correction).

In order to accomplish this conversion, the change in length of a vessel side, bottom, or end resulting from a deformation caused by pressure applied in the center of the plane was calculated. This deformation causes a change in the strain patch output depicted as follows:

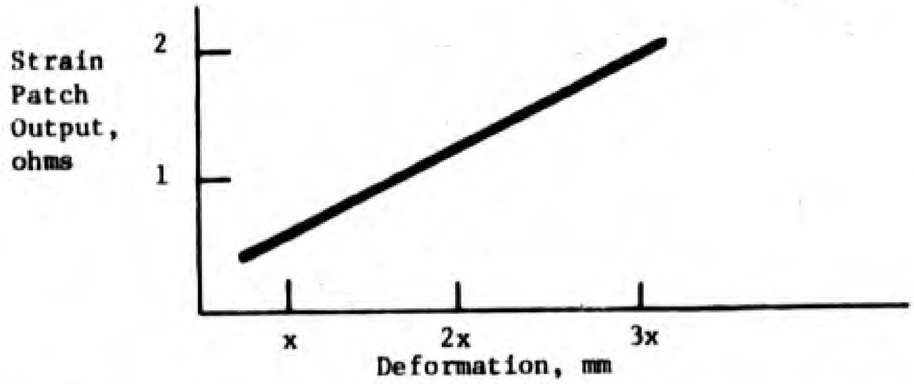

The output was correlated to the pressure determined from the model. This is graphically represented as

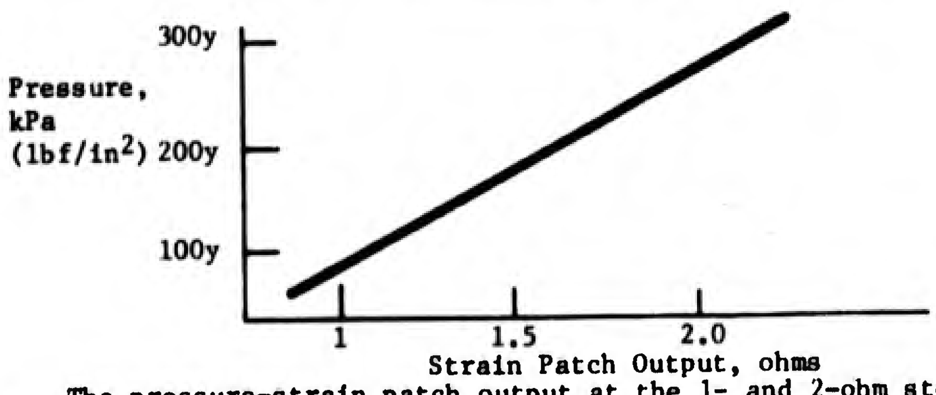

The pressure-strain patch output at the 1- and 2-ohm steps was plotted for each distinct plane of the test vessel and a gage factor was determined. The pressure was then computed from:

$$p = \frac{\text{height of pressure peak}}{\text{height of 2 ohm step}} \times \text{gage factor}$$

The computed pressure from this method was compared to pressure computed from the model by substituting a measured permanent deformation from half-scale vessels that did not fail. The paired points (measured/calculated)are 167/173, 76/67 and 74/71. These values agree to within approximately 3.5, 11.1 and 4.1 percent, respectively. Because of the limited data, no bias could be determined.

During testing, the observation was made that the bottom and side strain patches were affected by counter movements of these planes upon pressurization. These movements resulted in a displacement of the base line upon ignition and during testing. As a result, only the end strain patch was used to determine results. This strain patch showed no shift in the base line that did not result from the reaction. The validity of these data as determined by another method is discussed in the results section of the report.

APPENDIX C

TYPICAL STRAIN-TIME CURVES

The typical traces exhibit a slow rise in pressure from 10 percent to about 50 percent maximum pressure. Beyond this point, the pressure rises rapidly, normally exhibiting more than two levels of rate. The maximum rise occurred between 80 and 100 percent maximum pressure on most tests (75 - 100 and 95 - 100 points were observed on two tests). The observation of sudden changes in slope immediately before failure was not observed (at least within a measurable time frame). This indicates that failure occurred - when a certain pressure was obtained - regardless of the rate of rise to achieve the required pressure. As a consequence, it is logical to assume that rate of rise was established and stable prior to rupture. Since this stable rise occurred in the terminal portion (80 - 100 percent) of the record, this time frame was selected for rate of rise measurement.

Typical Strain-Time Curves

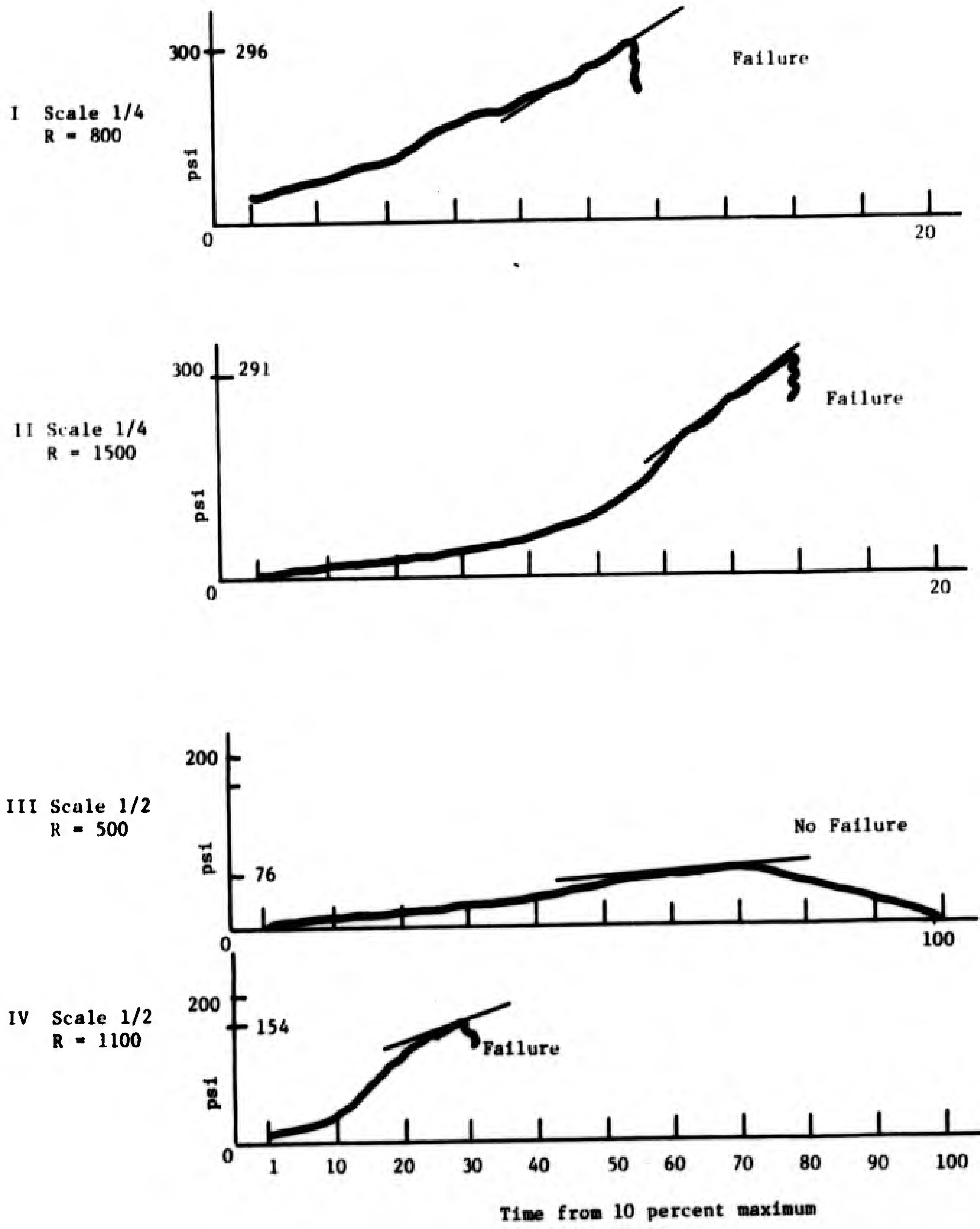

MODEL ANALYSIS OF PROPELLANT BURNING IN VENTED CHAMBER

W. E. Baker
Southwest Research Institute
San Antonio, TX

These notes refer to scaling of tests of M26 and M30 propellants in a vented drying oven. The full scale oven is a long horizontal chamber of roughly rectangular box configuration, 20 ft long by 3½ ft wide by 2 ft deep. Propellants fill about 6 in. depth in the chamber during drying, and the lid has a number of light blowout panels for venting. Properties of the two propellants are given in Table 1. About 1500 lb of propellant are in the drying oven.

TABLE 1. PROPELLANT PROPERTIES

Propellant	M-30 (triple-base)	M-26 (double-base)
Specific energy, cal/g	1000	1000
Geometry of grains		
Perforations	7	7
Length, in.	0.643	0.447
Diameter, in.	0.304	0.203
Web thickness, in.	0.058	0.037
Specific weight, lb/in^3	0.060	0.058
Specific surface area, ft^2/lb_m	2.832	4.54
Packing fraction	0.8-0.9	0.8-0.9
Pressure coefficient*, c	0.0050	0.00083
Pressure exponent*, n	0.68	0.87

*Units and dimensions of these quantities will be discussed later.

The primary purpose of model-scale tests is to verify whether these propellants are indeed Class 2 (fire) hazards only in this dryer, as believed from preliminary tests. But, a secondary purpose is to obtain data on scaling to verify the applicability of small-scale ignition and burning tests. In the tests, pressure-time histories, or strain-time histories which can be translated into pressure-time histories, will be the primary instrumentation.

The model analysis given here applies to the processes of propellant burning, pressure and temperature rise in the vented chamber, and the venting process. It does not include static or dynamic response of the chamber itself, although scaling of such response could be included in an extended analysis.

The first step in this (or any) model analysis is to list the physical parameters one feels to be important and give their dimensions. We will use a force, length, time, temperature (F, L, T, θ) system of units in listing dimensions. Based on our discussions with Radford and Picatinny personnel regarding this problem, we list the large number of parameters (24) in Table 2 as potentially important in this problem. In most cases, the dimensions are self-evident, but the parameters a and b should be discussed. Radford personnel indicated that linear burning rate r is given empirically by

$$r = c\,p^{n} \tag{1}$$

where c and n are empirical coefficients obtained from closed-bomb testing. Values of these coefficients are given in Table 1. But, for the low pressures almost sure to apply in these well-vented tests, eq. (1) says that the burning rate is zero for zero pressure. This is a physically unrealistic result. We choose instead to use the empirical equation

$$r = a + b\,p \tag{2}$$

which gives a finite burning rate for zero pressure. To maintain dimensional homogeneity in eq. (2), the coefficients must have dimensions*

$$\begin{aligned} a &\overset{d}{=} L/T \\ b &\overset{d}{=} L^3/FT \end{aligned} \tag{3}$$

---

*The symbol " $\overset{d}{=}$ " means "dimensionally equal to."

TABLE 2. PHYSICAL PARAMETERS AND DIMENSIONS

Symbol	Parameter	Dimensions
V_v	Chamber volume	L^3
V_p	Propellant volume	L^3
A	Vent area	L^2
$p(t)$	Pressure in chamber	F/L^2
p_a	Outside ambient pressure	F/L^2
E	Propellant total energy	FL
Q	Propellant mass burning rate	$M/T = FT/L$
r	Propellant linear burning rate	L/T
$\dot{p} = dp/dt$	Pressure rate	F/L^2T
e	Propellant specific energy	$FL/M = L^2/T^2$
γ_p	Specific heat ratio for propellant gas	—
γ_a	Specific heat ratio for air	—
d	Packing fraction	—
L	Characteristic length	L
ℓ_i	Length ratios	—
t	Time	T
a_a	Sound velocity in air	L/T
a_p	Sound velocity in propellant gas	L/T
S	Specific surface area of propellant	$L^2/M = L^3/FT^2$
θ_p	Propellant burn temperature at constant pressure	θ
θ_v	Propellant burn temperature at constant volume	θ
θ_i	Initial propellant temperature	θ
a, b	Coefficients in burning rate equation	L/T, L^3/FT

The next step in a model analysis is the formation of a number of dimensionless groups, or pi terms, from the list of physical parameters. The number of groups formed equals the number of parameters less the number of basic physical dimensions; here 24 - 4 = 20. One possible set of pi terms is given in Table 3.

Strictly speaking, Table 3 is the <u>model law</u> for this problem. For strict scaling, <u>all</u> parameters in Table 3 must remain invariant in tests at any scale for the law to be satisfied. In reality, we must usually compromise and violate equality of one or more pi terms. It is helpful next to show the relations between scale factors for various physical quantities imposed by Table 3, and then consider further limitations imposed by the real world.

Let us call scale factors λ_A, where λ is the ratio of the physical parameter A in sub-scale to the same parameter full-scale. Then, Table 3 requires that:

$$\lambda_{V_v} = \lambda_{V_p}$$

$$\lambda_A = \lambda_{V_v}^{2/3}$$

$$\lambda_p = \lambda_{p_a}$$

$$\lambda_E = \lambda_{p_a}\lambda_{V_v}$$

$$\lambda_Q\lambda_{a_a} = \lambda_{p_a}\lambda_{V_v}^{2/3}$$

$$\lambda_{\dot{p}}\lambda_{V_v}^{1/3} = \lambda_{a_a}\lambda_{p_a} \qquad (4)$$

$$\lambda_e = \lambda_{a_a}^2$$

$$\lambda_{\gamma_a} = \lambda_{\gamma_p} = \lambda_{\ell_1} = \lambda_d = 1$$

$$\lambda_L = \lambda_{V_v}^{1/3}$$

$$\lambda_t\lambda_{a_a} = \lambda_{V_v}^{1/3}$$

$$\lambda_{a_p} = \lambda_{a_a} = \lambda_r$$

(continued)

TABLE 3. PI TERMS FOR PROPELLANT BURNING AND VENTING

Number	Term
π_1	(V_p/V_v)
π_2	$(A/V_v^{2/3})$
π_3	(p/p_a)
π_4	$(E/p_a V_v)$
π_5	$(Qa_a/p_a V_v^{2/3})$
π_6	$(\dot{p} V_v^{1/3}/a_a p_a)$
π_7	(e/a_a^2)
π_8	γ_p
π_9	γ_a
π_{10}	$(L/V_v^{1/3})$
π_{11}	ℓ_i
π_{12}	$(ta_a/V_v^{1/3})$
π_{13}	(a_p/a_a)
π_{14}	(r/a_a)
π_{15}	$(Sp_a V_v^{1/3}/a_a^2)$
π_{16}	(θ_p/θ_i)
π_{17}	(θ_v/θ_i)
π_{18}	(a/a_a)
π_{19}	(bp_a/a_a)
π_{20}	d

$$\lambda_{\dot{S}}\lambda_{p_a}\lambda_{V_v}^{1/3} = \lambda_{a_a}^2$$

$$\lambda_{\theta_p} = \lambda_{\theta_v} = \lambda_{\theta_i} \qquad (4)$$

$$\lambda_a = \lambda_{a_a}$$

$$\lambda_b\lambda_{p_a} = \lambda_{a_a}$$

Now, assume that model-and full-scale tests are run in the same atmosphere. This means that

$$\lambda_{p_a} = \lambda_{a_a} = \lambda_{r_a} = \lambda_{\theta_i} = 1 \qquad (5)$$

This reduces the set of relations (4) to

$$\lambda_{V_v} = \lambda_{V_p}$$

$$\lambda_A = \lambda_{V_v}^{2/3}$$

$$\lambda_p = 1$$

$$\lambda_E = \lambda_{V_v}$$

$$\lambda_Q = \lambda_{V_v}^{2/3} \qquad (6)$$

$$\lambda_{\dot{p}}\lambda_{V_v}^{1/3} = 1$$

$$\lambda_e = 1$$

$$\lambda_{Y_p} = \lambda_{\ell_i} = \lambda_d = 1$$

$$\lambda_L = \lambda_{V_v}^{1/3}$$

(continued)

$$\lambda_t = \lambda_{V_v}^{1/3}$$
$$\lambda_{a_p} = \lambda_r = 1$$
$$\lambda_S \lambda_{V_v}^{1/3} = 1 \qquad (6)$$
$$\lambda_{\theta_p} = \lambda_{\theta_v} = 1$$
$$\lambda_a = 1$$
$$\lambda_b = 1$$

Several of these factors can only be satisfied if we use the <u>same</u> propellant in model and full scale tests, i.e., $\lambda_r = \lambda_{a_p} = \lambda_{\gamma_p} = \lambda_e = \lambda_a = \lambda_b = 1$. This requirement also makes $\lambda_S = 1$. Using this limitation and eliminating scale factors which are then automatically satisfied, such as $\lambda_E = \lambda_{V_v}$ (total energy proportional to total volume), and introducing the notation $\lambda = \lambda_L$,

$$\lambda_{V_v} = \lambda_{V_p} = \lambda^3$$
$$\lambda_A = \lambda_V^{2/3} = \lambda^2$$
$$\lambda_p = 1$$
$$\lambda_Q = \lambda_{V_v}^{2/3} = \lambda^2$$
$$\lambda_{\dot{p}} = 1/\lambda \qquad (7)$$
$$\lambda_{\ell_i} = \lambda_d = 1$$
$$\lambda_r = 1$$
$$\lambda_t = \lambda$$
$$\lambda_S \lambda = 1$$
$$\lambda_{\theta_p} = \lambda_{\theta_v} = 1$$

It is possible to satisfy all but one of the scale factor relations in (7) with a so-called "replica" model, which employs exactly the same geometry as in full-scale, and shrinks the time scale by the geometric scale factor λ. The relation which is not properly scaled is enclosed in a box in eq. (7) and is

$$\lambda_S = 1/\lambda \tag{8}$$

This quantity does not scale because the propellant grains are not scaled between model and full-scale, but instead are identical. Thus, S is not changed as the scale of the experiment changes, but instead remains constant. Whether or not failure to scale this one quantity is important can only be determined by conducting tests at different scales.

The implications of the scaling law, with the limitation noted above, are as follows:

(1) Scale model tests with a geometry exactly similar to full-scale, including scaling of linear dimensions of vents, should produce the same pressures and temperatures in the model as would be experienced full-scale, at times compressed by the linear geometric scale factor λ.

(2) Pressure rates $\dot{p}$ are faster in the model tests because this quantity scales as $1/\lambda$.

(3) Mass burning rate Q scales as λ^2.

(4) Vent area is most conveniently expressed in the dimensionless form given by π_2, i.e., $(A/V_v^{2/3})$.

A series of tests conducted at various scale factors should verify or disprove this law. The one factor which is not properly scaled is the specific surface area of the propellant. The tests at different scales should, if properly conducted and instrumented, determine whether failure to scale this one quantity is important. If so, the test results may well determine a correction factor which can be used to predict full-scale results.

DISTRIBUTION LIST

Commander
US Army Armament Research and
Development Command
ATTN: DRDAR-CG
DRDAR-LC
DRDAR-LCM
DRDAR-LCM-S (12)
DRDAR-SF
DRDAR-TSS (5)
DRDAR-LCU-P
Dover, NJ 07801

Commander
US Army Materiel Development
and Readiness Command
ATTN: DRCDE
DRCIS-E
DRCPA-E
DRCPP-I
DRCDL
DRCSG-S
5001 Eisenhower Avenue
Alexandria, VA 22333

Commander
USDRC Installations & Services Agency
ATTN: DRCIS-RI-IU
DRCIS-RI-IC
Rock Island, IL 61299

Commander
US Army Armament Materiel and
Readiness Command
ATTN: DRSAR-IR (2)
DRSAR-IRC
DRSAR-ISE (2)
DRSAR-IRC-E
DRSAR-PDM
DRSAR-LC (2)
DRSAR-ASF (2)
DRSAR-SF (3)
DRSAR-LEP-L
Rock Island, IL 61299

Chairman
Dept. of Defense Explosives Safety Board
Hoffman Bldg 1, Rm 856C, 2461 Eisenhower Ave.
Alexandria, VA 22331 (2)

Project Manager for Munition Production
Base Modernization and Expansion
ATTN: DRCPM-PBM-LA
DRCPM-PBM-T-SF
DRCPM-PBM-EP (2)
Dover, NJ 07801

Director
Ballistic Research Laboratory
ARRADCOM
ATTN: DRDAR-BLE (C.Kingery)
Aberdeen Proving Ground, MD 21010 (2)

Defense Documentation Center
Cameron Station
Alexandria, VA 22314 (12)

Commander
US Army Construction Engineering
Research Laboratory
ATTN: CERL-ER
Champaign, IL 61820

Office, Chief of Engineers
ATTN: DAEN-MCZ-E
Washington, DC 20314

US Army Engineer District, Huntsville
ATTN: Construction Division-HAD-ED (2)
P.O. Box 1600 West Station
Huntsville, AL 35807

Commander
Indiana Army Ammunition Plant
ATTN: SARIN-OR (2)
SARIN-SF
Charlestown, IN 47111

Commander
Kansas Army Ammunition Plant
ATTN: SARKA-CE
Parsons, KS 67537

Commander
Lone Star Army Ammunition Plant
ATTN: SARLS-IE
Texarkana, TX 57701

Commander
Milan Army Ammunition Plant
ATTN: SARMI-S
Milan, TN 38358 (5)

Commander
Radford Army Ammunition Plant
ATTN: SARRA-IE (2)
Radford, VA 24141

Commander
Badger Army Ammunition Plant
ATTN: SARBA (2)
Baraboo, WI 53913

Commander
Holston Army Ammunition Plant
ATTN: SARHO-E
Kingsport, TN 37662

Weapon System Concept Team/CSL
ATTN: DRDAR-ACW
Aberdeen Proving Ground, MD 21010

Technical Library
ATTN: DRDAR-CLJ-L
Aberdeen Proving Ground, MD 21005

Technical Library
ATTN: DRDAR-TSB-S
Aberdeen Proving Ground, MD 21010

Technical Library
ATTN: DRDAR-LCB-TL
Benet Weapons Laboratory
Watervliet, NY 12189